PSF (not shown). When fitted with uniform weighting, however, these FWHM data from the Pearson VII PSF fell quite precisely (not shown) on the simulated curve. Below 40° 2θ, a split PSF will provide results that over-estimate true FWHM values, as shown in Figs. 3.1.27 and 3.1.31. The cause for this is analogous to that discussed for the $\Delta(2\theta)$ values, and can be readily observed in the fit quality displayed in Fig. 3.1.32 for the low-angle 100 reflection. In accounting for the asymmetry to low angle, the FWHM of the observed profile is substantially overestimated by the calculated one. With all PSFs, the high-angle FWHM values are observed to be over-estimated, as shown in Figs. 3.1.27 and 3.1.31; the problem is exacerbated with the use of the Caglioti function. Inspection of the fit quality of the high-angle 510 line shown in Fig. 3.1.32 indicates that there are two contributions to this effect: one is that the PSF cannot model the shape of the high side of the profile; the other is that the height of the profile is underestimated. These two effects, particularly the inability of the PSF to correctly model the height of the profile, were observed with all of the other PSFs considered here.

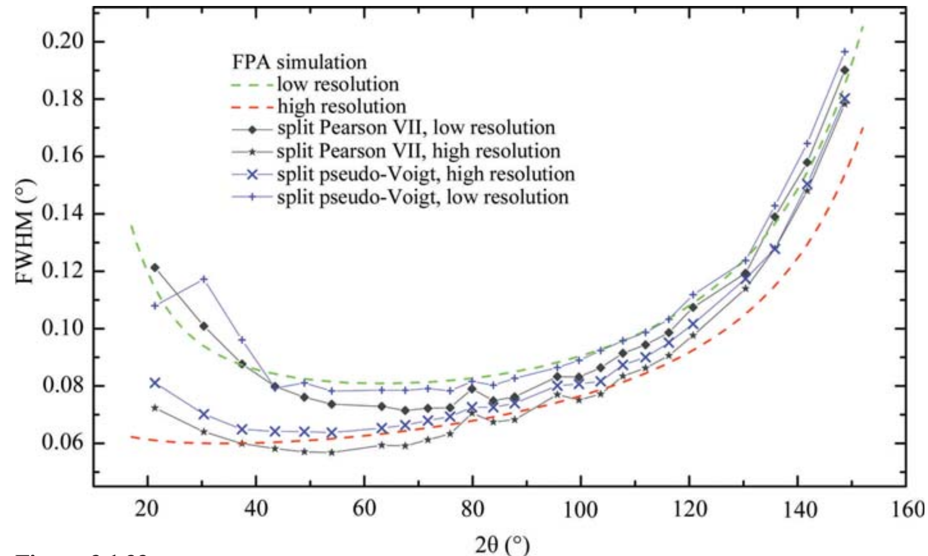

Figure 3.1.33
FWHM data from fits of the split pseudo-Voigt and split Pearson VII PSFs to simulated low- and high-resolution data.

The use of the pseudo-Voigt PSF with the Caglioti function results in a reasonable fit to the FWHM values of the observation; however, the breadth of the high-angle lines is over-estimated. The *U*, *V* and *W* terms of the Caglioti function vary in a specific manner to account for various physical effects (*e.g.* see Fig. 3.1.27): the *U* term, in tan θ, accounts for angular dispersion; the *W* term describes the 'floor' and the *V* term accounts for the reduction of the FWHM values in the mid-2θ region. Therefore, the *U* and *W* terms should refine to positive values, while the *V* term should tend to a negative value; negative values for *V* were, indeed, obtained in these analyses. *V* should be constrained to negative values or set to zero, as positive values for *V* are non-physical. With an instrument configured for high resolution, however, values of $V = 0$ are entirely reasonable as the trend towards an upturn in FWHM at low 2θ angle will be suppressed.

To some extent, the difficulties in determining profile positions through the use of these PSFs can be ascribed to the Cu $K\alpha_1/K\alpha_2$ doublet as it is stretched by angular dispersion. The pattern can be thought of as divided into three regions, each of which will confound fitting procedures in a different manner: the low-2θ range, where profiles can be considered as a peak with a shoulder, the mid-2θ range (perhaps 40 to 110° 2θ), where the profiles can be considered as a doublet, and the high-angle region where they are two distinct peaks. This 'three-region' consideration is compounded by the direction and severity of the asymmetry in these profiles. The data shown in Fig. 3.1.27 largely correspond to the problematic effects of angular dispersion in the context of these three 2θ regions. These effects are particularly apparent, as shown in Fig. 3.1.31, with the use of the Pearson VII function: over-estimation of FWHM values occurs at low 2θ, under-estimation occurs in the mid-2θ region, and credible values are obtained at high angle. The use of the Caglioti function is effective in addressing the more extreme excursions from plausible FWHM values. Fig. 3.1.28 shows the left and right HWHM values for SRM 660b using the split pseudo-Voigt PSF refined with uniform weighting. For reasons discussed in Section 3.1.2, the degree, direction and point of crossover in the profile asymmetry indicated in Fig. 3.1.28 are in correspondence with expectation and the previously discussed results from these data from SRM 660b.

To consider the impact of instrument resolution on the use of analytical PSFs for the determination of FWHM values, the simulated high-resolution and low-resolution data were analysed *via* profile fitting. Fig. 3.1.33 shows the results from the use of the split Pearson VII and spilt pseudo-Voigt PSFs. The data of Fig. 3.1.33 indicate an effect that is dependent on the PSF used. The performance of the split Pearson VII PSF is observed to improve with instrument resolution; FWHM values from the narrower profiles are observed to correspond with expectation in the low- and mid-angle regions, while substantial deviation is noted with the broader profiles. This is counter to expectation, as broader profiles are generally easier to fit than narrow ones. The performance of the split pseudo-Voigt PSF is observed to degrade marginally with either an increase or decrease in instrument resolution. Curiously, the breadths of the profiles in the high-resolution data are overestimated, while those in low-resolution data are largely underestimated. Both PSFs do quite poorly in fitting the high-angle data from the high-resolution setting. These observations emphasize the need to scrutinize the results with an examination of the fit quality, as per Fig. 3.1.32.

When the IPF is simplified with the use of a Johansson IBM, analytical PSFs can provide an excellent fit to the observations. Fig. 3.1.34 shows the fit quality of the split Pearson VII PSF to (high-quality) peak-scan data. The split Pearson VII PSF consistently provides a better fit to IBM data than either the split Voigt or split pseudo-Voigt PSFs. Note that the asymmetry exhibited by the profiles follows the same trends as were outlined previously, but to a much reduced extent because of the extended incident-beam path length and the resulting reduction in the effects of axial divergence. Fig. 3.1.35 shows the $\Delta(2\theta)$ calibration curves that were obtained as per the procedures outlined for Fig. 3.1.29. Indeed, the trends that are followed, and the reasons why, are largely analogous to those of Fig. 3.1.29, but to a much reduced extent because of the reduced profile asymmetry. Use of symmetric PSFs yields reported peak positions that are shifted in the direction of the asymmetry, while use of split PSFs yields positions shifted in the opposite direction owing to the fitted profiles displaying excessive levels of asymmetry. One notes the complete failure of the split pseudo-Voigt, split Voigt (not shown)

  references